

## Section 2

# PROGRESS IN LASER FUSION

### 2.A Harmonic Radiation from IR- and UV-Laser Plasmas

In order to optimize the coupling of laser light to laser-fusion targets, it is necessary to understand the basic laser-plasma interaction processes taking place in the plasma corona at densities up to the critical density. There the electron plasma frequency,  $\omega_p$ , equals the laser frequency,  $\omega_o$ , thus shielding the target interior from laser irradiation. All interaction processes depend to varying degrees on coronal parameters such as density, density gradients, coronal electron temperature, and plasma flow velocity. Thus, there is a premium on coronal diagnostics as well as on direct or indirect experimental signatures of the individual interaction processes.

A number of these interaction processes take place at or near the critical density (resonance absorption, parametric-decay instability) or the quarter-critical density [absolute Raman instability (SRS) and two-plasmon ( $2\omega_p$ ) instability]. These processes typically involve the generation of one or more plasma waves with frequencies close to either  $\omega_o$  (at  $n_c$ ) or  $\omega_o/2$  (at  $n_c/4$ ). These plasma waves ("plasmons") can reradiate electromagnetic (e-m) waves in various ways, either through a combination of one, two, or more plasmons, or through scattering of incident photons from these plasma waves. The frequencies of the e-m waves generated in this way are typically multiples of half the laser frequency. Thus, many of the primary interaction processes can be diagnosed through the observation of the harmonic radiation emitted by the

plasma. Moreover, this radiation contains spectral details which relate to the coronal plasma conditions in the case of the odd-integer half-harmonics, while details of primary and secondary decay processes near  $n_c$  may be studied in the harmonics of the fundamental laser frequency.

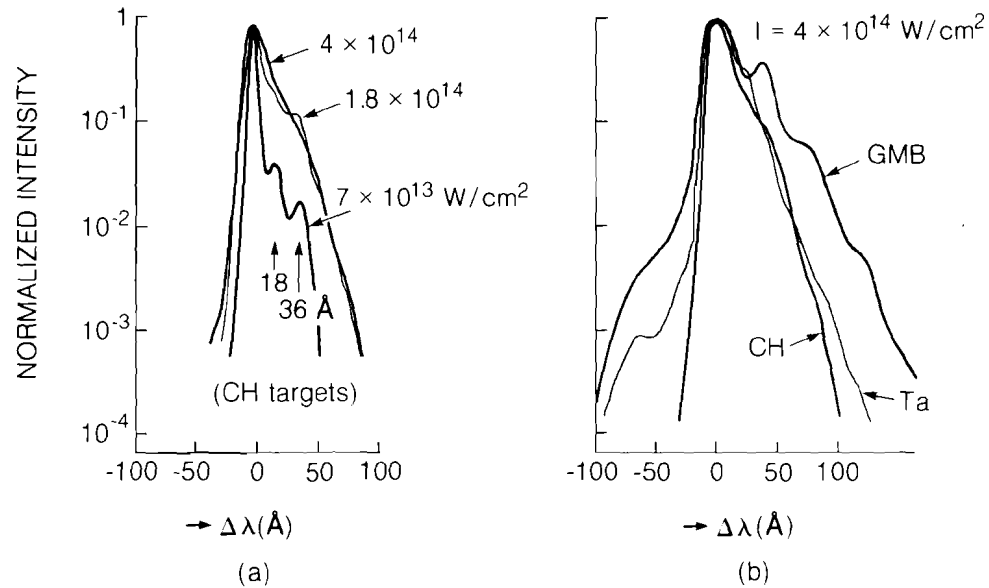
Thus, the interest in studying harmonic radiation from laser plasmas is twofold: we gain information on the laser-plasma interaction processes as well as on the plasma conditions in the interaction region. Furthermore, detailed understanding of these processes can shape and significantly influence future laser-plasma and laser-fusion experiments.

Over the past two years, we have investigated a number of laser-plasma interaction processes in UV- and IR-laser plasmas. We have observed a number of half-harmonics of the laser frequency, such as  $\omega_0/2$ ,  $3\omega_0/2$ ,  $2\omega_0$ , and  $5\omega_0/2$ . Not all harmonics could be observed under all irradiation conditions; in the UV experiments no spectra beyond the  $3\omega_0/2$  harmonic were examined, while in the IR experiments the  $\omega_0/2$  harmonic was only poorly resolved due to instrumental difficulties in this wavelength regime ( $2\mu\text{m}$ ).

Harmonics of the fundamental irradiation frequency have been observed in laser plasmas for a long time.<sup>1</sup> The longer the irradiation wavelength, the higher the harmonics that have been observed.<sup>2</sup> In  $1\text{-}\mu\text{m}$  irradiation the second harmonic is the principal integer harmonic observed. An excellent survey on second-harmonic generation and the underlying laser-plasma interaction processes has been published by Basov *et al.*<sup>3</sup> Two laser-plasma interaction processes are primarily responsible for the emission of multiples of the fundamental frequency, in particular the second harmonic. The first process, resonance absorption, involves linear conversion of incident photons into plasmons at  $n_c$ . This process does not have a threshold and is more efficient for obliquely incident p-polarized light than for s-polarized light.<sup>4</sup> The second process, the parametric-decay instability, occurs just below  $n_c$ ; the incident e-m wave decays into a plasma wave and an ion-acoustic wave whose k-vectors are approximately parallel to the E-vector of the e-m wave, i.e., normal to the density gradient. Typical thresholds for this instability lie just below  $10^{14}\text{ W/cm}^2$  for long-pulse (ns) IR irradiation. Evidence for this instability has been described in Refs. 3 and 5.

### Second-Harmonic Spectra

Second-harmonic spectra obtained from OMEGA experiments (with  $\lambda_L = 1.05\ \mu\text{m}$ ) have shown more details than hitherto reported (see Fig. 1). The reason for this greater spectral clarity is probably related to OMEGA's high degree of irradiation uniformity ( $\leq 10\%$  rms variation) which surpasses that of earlier experiments. We note that the second-harmonic spectra typically contain a main peak with subsidiary lower-intensity peaks spaced by approximately  $19\ \text{\AA}$  from each other to the red side of the main peak.



E2537

Fig. 1

Second-harmonic spectra from IR-laser plasmas. Spherical targets of various materials were irradiated in OMEGA with 24 beams for 1 ns at  $1.05 \mu\text{m}$ . (a) Intensity dependence of spectra from solid CH spheres. (b) Target material (target-Z) dependence of spectra obtained by irradiating massive spherical targets at  $10^{14} \text{W/cm}^2$ .

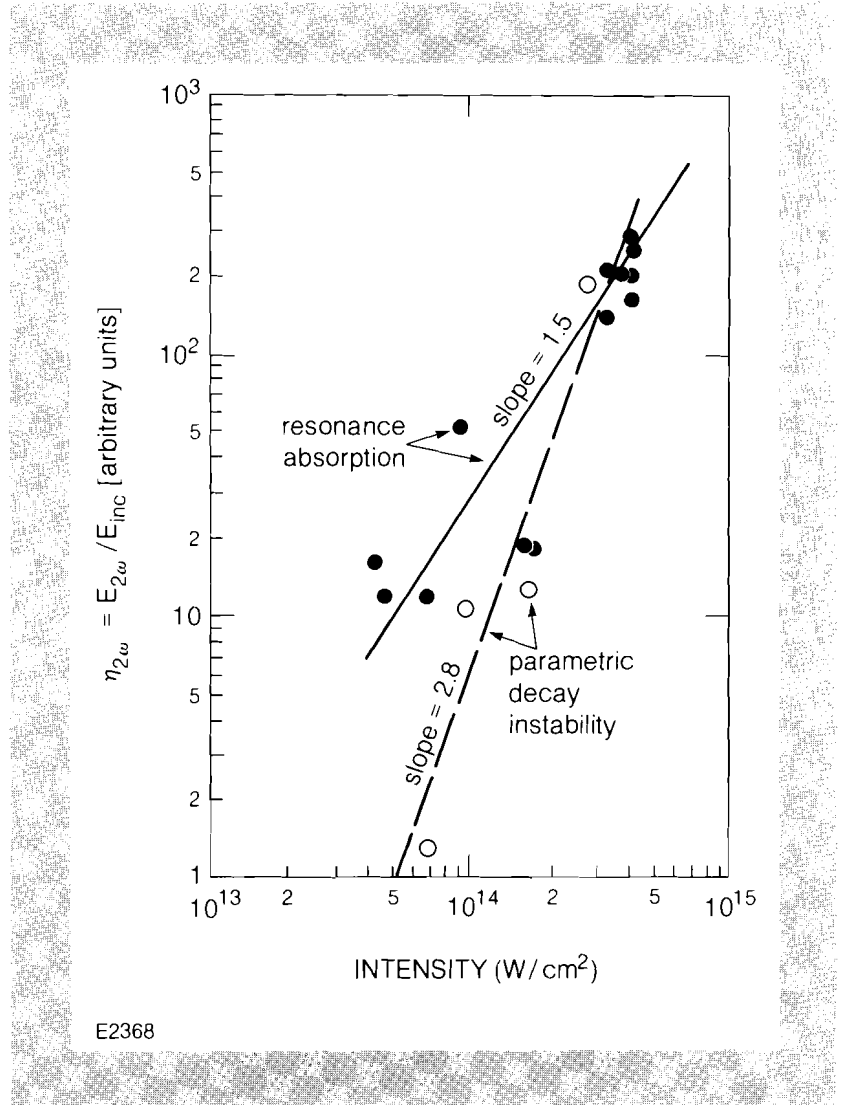
The main peak is traditionally identified with the existence of resonance absorption at  $n_c$ . Second-harmonic photons can be produced either by scattering of incident photons from the plasmons produced by resonance absorption or by two-plasmon-to-photon reconversion. From the polarization of this second-harmonic emission, we believe that scattering is the more likely process. The dependence of the  $2\omega$  emission on angle of incidence and polarization (p or s with respect to the plane of incidence) has led to clear identification of this spectral feature as a signature of resonance absorption. The intensity dependence of this spectral feature is expected to be

$$I_{2\omega}^{\text{RA}} \propto I_{\omega}^2, \text{ or } \eta_{2\omega}^{\text{RA}} \equiv I_{2\omega} / I_{\omega} \propto I_{\omega}.$$

In Fig. 2 we have plotted the experimentally observed intensity scaling of the main peak of the  $2\omega$  radiation relative to the incident radiation. The observed scaling is stronger than expected. This discrepancy may be explained by the intensity dependence of inverse-bremsstrahlung absorption: at lower intensities where the absorption is high the intensity at critical is substantially reduced from the incident intensity. Estimates of this effect have shown that the observed scaling is easily explained in this way.

The locations of the peaks on the red side of the main  $2\omega$  peak in Fig. 1 are apparently independent of either intensity (and therefore temperature) or target material (target Z). Furthermore, these side peaks are only seen above a certain irradiation intensity

Fig. 2  
Intensity dependence of the main  $2\omega$  peak (solid circles) and the first red side peak (open circles). The main peak is due to scattering of incident photons on plasmons created by resonance absorption at  $n_c$ . The intensity scaling (solid line) is faster than expected due to the intensity dependence of inverse-bremsstrahlung absorption. The intensity of the side peak (dashed line) shows the predicted intensity behavior<sup>3</sup> of the parametric-decay instability if the intensity dependence of inverse-bremsstrahlung absorption is taken into account.



( $I \geq 5 \times 10^{13}$  W/cm<sup>2</sup>). Their intensities relative to the main  $2\omega$  peak rise with increasing irradiation intensity (see Fig. 2),

$$I_{2\omega}^{\text{PD}} / I_{\omega} \propto I_{\omega}^{2.8},$$

in close agreement with predictions made in Ref. 3 if allowance is made for the nonlinearly increased laser intensity at critical due to the intensity dependence of inverse-bremsstrahlung absorption. The generation of this radiation involves the combination of two plasmons generated by the parametric-decay instability just below  $n_c$ . At intensities above  $4 \times 10^{14}$  W/cm<sup>2</sup> the detailed structure of these side peaks merges into a continuum and saturates below the level of the main  $2\omega$  peak. In some cases, similar side peaks are found on the blue side of the main  $2\omega$  peak, though their intensities are approximately one order of magnitude below those of the red peaks. The peaks on the blue side are most easily seen for glass targets although they have also been seen for other targets under certain conditions. The blue substructure reported here is

much more detailed than reported previously.<sup>3</sup> Existing theory does not explain these blue-shifted peaks, though their splitting of twice that of the red substructure would appear to point to a related mechanism.

### Odd-Integer Half-Harmonic Spectra

Spectra of the  $3\omega_o/2$  emission have been observed for a long time.<sup>6</sup> The reason for the occurrence of  $3\omega_o/2$  emission and other odd-integer half-harmonics lies in the existence of laser-driven instabilities at  $n_e = n_c/4$ , where  $\omega_p = \omega_o/2$ . At this density, the incident wave may be subject to either of two resonant decay processes, the absolute stimulated-Raman-scattering instability (SRS) and/or the  $2\omega_p$ -decay instability. In the former, the incident e-m wave decays into a scattered e-m wave and a plasma wave, both of frequency  $\omega_s \approx \omega_p \approx \omega_o/2$ , while in the  $2\omega_p$ -decay instability the incident e-m wave decays into two plasma waves with  $\omega_p \approx \omega_o/2$ . Due to the energy, momentum, and dispersion relations [Eq. (1)] the exact frequencies differ slightly from  $\omega_o/2$ , and the directions of the daughter waves also depend on the exact process involved as well as on the laser intensity. The wave-matching conditions and dispersion relations are given by:

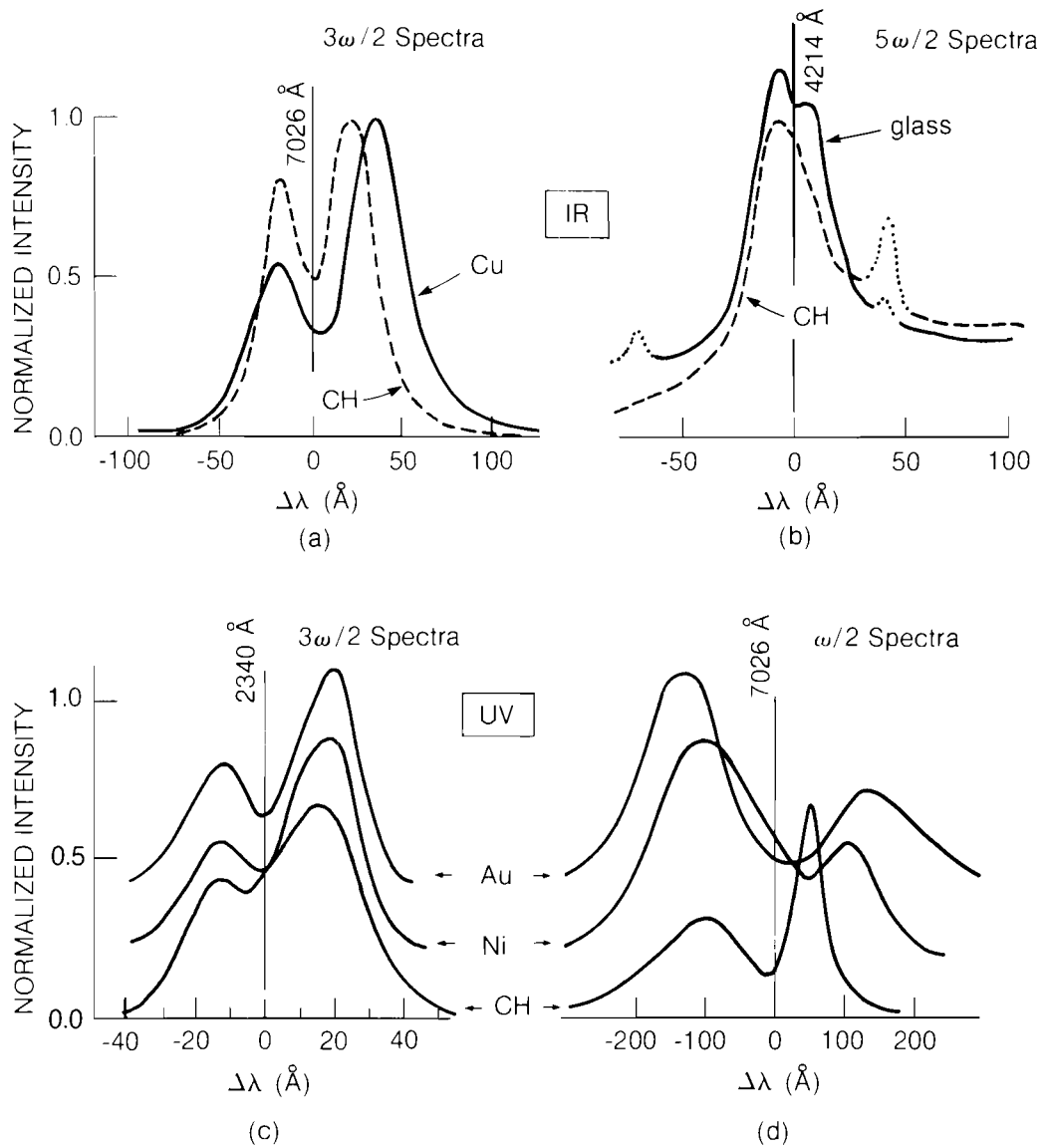
$$\begin{aligned}\omega_o &= \omega_{p1} + \omega_{p2} \\ \mathbf{k}_o &= \mathbf{k}_{p1} + \mathbf{k}_{p2} \\ \omega_o^2 &= \omega_{pe}^2 + c^2 k_o^2 \\ \omega_p^2 &= \omega_{pe}^2 + 3v_T^2 k_p^2,\end{aligned}\tag{1}$$

where  $\omega_{pe}$  is the electron plasma frequency and  $v_T (= \sqrt{kT_e/m_e})$  is the electron thermal velocity.

Typical odd-integer half-harmonic spectra are shown in Fig. 3. All of these spectra are generated by processes involving at least one of the plasmons generated at quarter critical. Typically, the  $2\omega_p$  instability has the lower threshold and furnishes the plasmons required. The generation of these harmonics at quarter critical could be due to conversion of one, three, or five plasmons to photons, Thomson scattering of incident laser light from the same plasmons (for  $\omega_o/2$  and  $3\omega_o/2$  emission), or Thomson scattering of  $2\omega$  photons produced at critical.

The splitting of the spectral lines observed at all odd-integer half-harmonics is due to the two plasma waves generated at  $n_c/4$  with frequencies just above and below  $\omega_o/2$ . The frequency difference is proportional to the coronal electron temperature and also depends on the k-vectors of the plasma waves. If the emission processes for  $\omega_o/2$ ,  $3\omega_o/2$ , and  $5\omega_o/2$  do not involve specific selections of plasma k-vectors, we may assume the splitting reflects the region of maximum growth of the  $2\omega_p$ -decay instability.<sup>7</sup> Then  $\Delta\omega$  is proportional to  $T_e f(k_{opt})$ , where  $k_{opt}$  is the plasma wave vector corresponding to the optimum growth rate of the instability and  $f(k) = [1 + 4(k/k_o)^2]^{1/2}$ .

Radiation at  $\omega_o/2$  can be produced either by SRS at  $n_c/4$  or by linear reconversion of  $2\omega_p$ -decay plasmons into photons in a



E2416

Fig. 3  
Odd-integer half-harmonic emission from IR- and UV-laser plasmas.

(a) and (b):  $3\omega_0/2$  and  $5\omega_0/2$  spectra from targets irradiated in OMEGA at 1 ns,  $1.05 \mu\text{m}$ , and  $4 \times 10^{14} \text{ W/cm}^2$ .

(c) and (d):  $3\omega_0/2$  and  $\omega_0/2$  spectra obtained from targets irradiated in GDL at 0.5 ns,  $0.35 \mu\text{m}$ , and  $4 \times 10^{14} \text{ W/cm}^2$ .

process which may be termed inverse resonance absorption. The former mechanism gives rise to a single red-shifted spectral component while the latter can give rise to red and blue components. In either case, the radiation should be polarized parallel to the incident laser light. The observed random polarization leads to the hypothesis that either the plasmons are scattered (randomized) prior to reconversion, or the  $\omega_0/2$  photons are scattered after creation in such a manner as will destroy their polarization. The former process appears more likely as it is also required to allow the lower-frequency plasma waves to reach their critical density or turning point where the reconversion can take

place. The angular emission pattern for this process depends strongly on the density-gradient scale length at  $n_c/4$ . For typical UV experiments with scale lengths of about  $50 \mu\text{m}$ , this implies that only plasmons with very small  $k_{\perp}$  can be converted.

Alternatively, filamentation of the laser beam inside the plasma may be invoked, opening another way of producing  $\omega_o/2$  radiation. The random polarization would then be a consequence of the steep radial density gradients inside the filaments. Angular emission patterns for this radiation have indeed shown indications of filamentation. However, while filamentation can easily explain the generation of the red component of the  $\omega_o/2$  spectrum, the generation of the blue peak presents difficulties.

The interpretation of the intensity scaling of the frequency splitting of the  $\omega_o/2$  spectra (Fig. 4) also presents a considerable challenge. The observed splitting is roughly proportional to the incident UV intensity, whereas we would expect it to be proportional to the coronal temperature, implying an approximate cube-root intensity scaling. Perhaps larger-angle plasmon scattering becomes more effective at higher intensities, thus allowing the inverse-resonance-absorption process to tap plasmons in different parts of the plasmon distribution depending on the incident intensity.

The  $3\omega_o/2$ -harmonic emission could be produced either by 3-plasmon conversion or by Thomson scattering of incident laser photons from  $2\omega_p$ -decay plasmons. We would expect the former process to lead to unpolarized emission, as in the case of the  $\omega_o/2$  conversion. However, this is contrary to what has been observed; furthermore, it appears unlikely that the clear, double-peaked spectrum seen in Figs. 3a and 3c would be observed in this case.

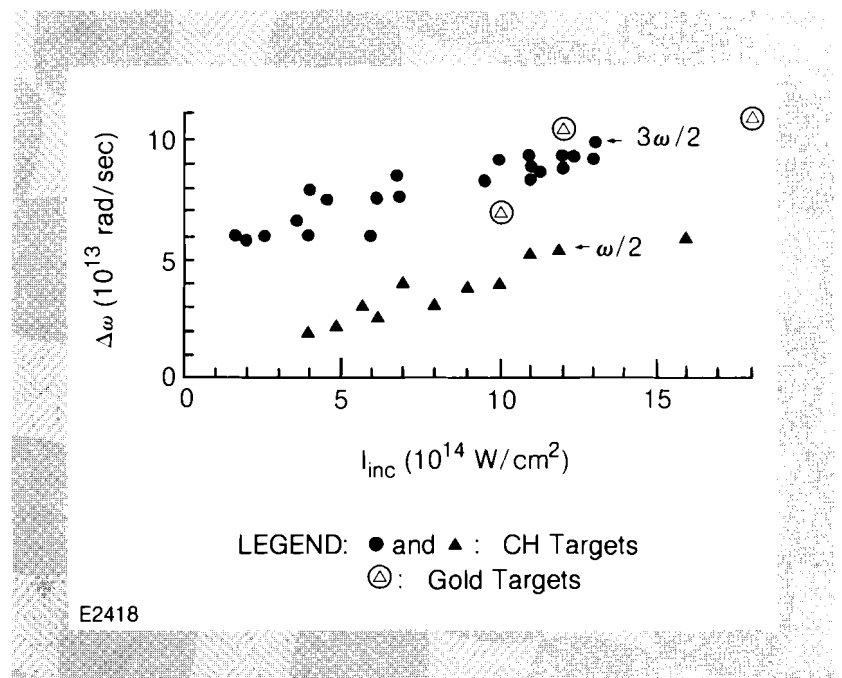


Fig. 4  
Frequency splitting of the 1/2- and 3/2-  
harmonic spectra from UV-laser plas-  
mas.

In contrast, the Thomson-scattering process preserves the polarization of the incident photons, but the random nature of the scattered  $2\omega_p$ -decay plasmons would lead to in-plane and out-of-plane scattering. This is indeed what we observe.

While the  $3\omega_o/2$ -harmonic splitting in IR experiments exhibits the expected double-peaked spectra symmetrically split around  $3\omega_o/2$ , the UV experiments show distinctly asymmetrical splitting (see Fig. 3c). Such asymmetry cannot be explained by existing theories at normal incidence. However, at oblique incidence such asymmetry may occur. Recent theoretical work at LLE indicates that the  $2\omega_p$ -decay instability may indeed occur with decreased thresholds inside self-focusing filaments which represent an extreme case of oblique incidence ( $90^\circ$  with respect to the density gradient). This configuration would also eliminate a difficulty encountered in the k-matching conditions for the  $3\omega_o/2$  scattering process in planar geometry for our UV experiments. This problem is related to the small plasma k-vector components perpendicular to the density gradient which have recently been predicted by Simon *et al.*<sup>7</sup> For typical IR-laser-plasma experiments Ref. 7 predicts  $k_\perp$ 's such that the  $3/2$ -harmonic radiation may be easily produced under most planar irradiation conditions without recourse to filamentation.

Comparing the theoretically predicted  $3\omega_o/2$  spectral splitting to that measured experimentally in UV- and IR-laser plasmas (Fig. 5), we note a very close agreement under IR-irradiation conditions while the agreement is much less close for UV irradiation. The latter may be a result of our plotting average intensities, since from other experimental evidence we know that the  $2\omega_p$ -decay instability occurs predominantly in the hot spots of the irradiated area. Thus, an arbitrary shift in the experimental intensity scale by a factor of 4-5 to higher intensities would resolve the discrepancy. On the other hand, the predicted spectra should be symmetrical around  $3\omega_o/2$  which they are not. The resolution of these problems may involve filamentation: preliminary calculations of  $3\omega_o/2$  generation inside filaments suggest that this effect may explain both the asymmetry and the magnitude of the spectral splitting.

The  $5\omega_o/2$  spectra observed in our IR-irradiation experiments on OMEGA have only been looked at in a cursory fashion. However, the frequency splittings of the  $5\omega_o/2$  and  $3\omega_o/2$  spectra in Fig. 3b are equal under equivalent experimental conditions, implying that the same plasma waves are involved in both processes. The  $5\omega_o/2$  scattering process could be viewed as Thomson scattering of  $2\omega$  photons on  $2\omega_p$ -decay plasmons at  $n_c/4$ . The  $2\omega$  photons would be produced by resonance-absorption plasmons as described earlier. The low level of  $5\omega_o/2$  radiation has precluded a systematic study to date, but its existence and generation mechanism appear well established. From images of spherically irradiated targets taken in  $3\omega_o/2$  and  $5\omega_o/2$  light, we have clearly established that the  $5\omega_o/2$  radiation does indeed come from the  $n_c/4$  surface.<sup>8</sup>

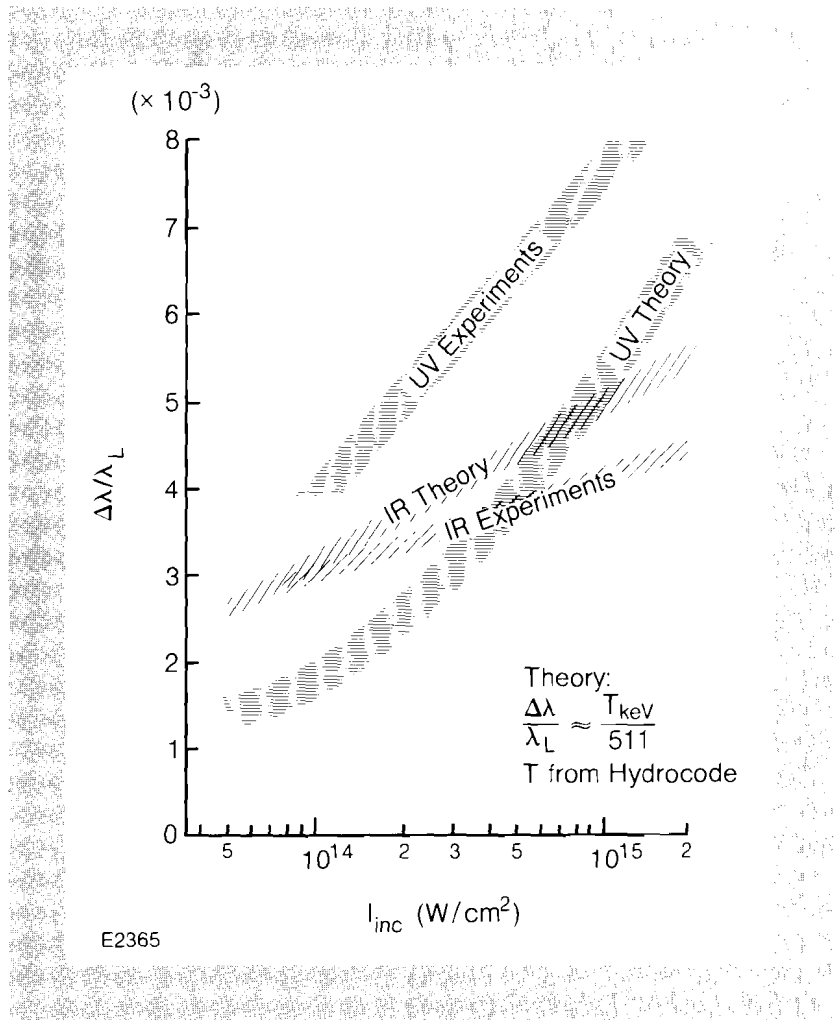


Fig. 5  
Intensity dependence of the splitting of 3/2-harmonic spectra from IR- and UV-laser plasmas. The UV data were obtained from planar CH targets irradiated in GDL ( $\lambda_i = 0.35 \mu\text{m}$ , 0.5 ns). The IR data were obtained on OMEGA with 1-ns, 24-beam symmetrical irradiation of solid CH spheres. The theoretical curves are obtained from temperatures predicted by hydrodynamic simulations and the formula  $\Delta\lambda/\lambda_i = T_{\text{keV}}/511$ .

**Conclusion**

We have observed a multitude of harmonics from IR- and UV-laser plasmas. Their generation mechanisms are generally well understood within the framework of existing theories, although detailed analyses require at times sophisticated extensions to these theories. In the relatively uniform plasmas produced by the 24-beam, 1.05- $\mu\text{m}$  OMEGA system the measured spectra are well matched by theoretical predictions. In the current UV experiments with their less uniform illumination the correlation with theory is not so close, particularly as regards the  $\omega_o/2$  spectra.

**REFERENCES**

1. A. Caruso, A. deAngeles, G. Gratti, R. Gratton, and S. Martellucci, *Phys. Lett.* **33A**, 29 (1970).
2. N. H. Burnett, H. A. Baldis, M. C. Richardson, and G. D. Enright, *Appl. Phys. Lett.* **31**, 172 (1977).
3. N. G. Basov, V. Yu. Bychenkov, O. N. Krokhin, M. V. Osipov, A. A. Rupasov, V. P. Silin, G. V. Sklizkov, A. N. Starodub, V. T. Tikhonchuk, and A. S. Shikanov, *Sov. Phys. JETP* **49**, 1059 (1979).